

Entanglement between Lowly and Highly Lying Atomic Spin Waves

D. S. Ding,^{1,2,*} K. Wang,^{1,2} W. Zhang,^{1,2} S. Shi,^{1,2} M. X. Dong,^{1,2}
Y. C. Yu,^{1,2} Z. Y. Zhou,^{1,2} B. S. Shi,^{1,2,†} and G. C. Guo^{1,2}

¹Key Laboratory of Quantum Information, University of Science and Technology of China, Hefei, Anhui 230026, China.

²Synergetic Innovation Center of Quantum Information and Quantum Physics,
University of Science and Technology of China, Hefei, Anhui 230026, China.

(Dated: May 19, 2021)

Establishing a quantum interface between different physical systems is of special importance for developing the practical versatile quantum networks. Entanglement between low- and high-lying atomic spin waves is essential for building up Rydberg-based quantum information engineering, otherwise be more helpful to study the dynamics behavior of entanglement under external perturbations. Here, we report on the successful storage of a single photon as a high-lying atomic spin wave in quantum regime. Via storing a K-vector entanglement between single photon and lowly lying spin wave, we thereby experimentally realize the entanglement between low- and high-lying atomic spin waves in two separated atomic systems. This makes our experiment the primary demonstration of Rydberg quantum memory of entanglement, making a primary step toward the construction of a hybrid quantum interface.

PACS numbers: 32.80.Ee,42.50.Nn,42.50.Gy

As a unique physical phenomenon in quantum mechanics, entanglement entails states of two or more objects that when separated cannot be described independently, a notion quite counterintuitive in classical physics. It plays a vital role in quantum-information engineering with separated entangled systems, and offers a great resource not available within classical counterparts, and it also be facilitative to study many fundamental quantum physics. In quantum information science, entanglement between separated physical systems is an indispensable resource in establishing distributed correlation across network nodes [1].

As the blockade effect of the large dipole moment of highly excited Rydberg atom in a confined volume [2, 3], a high-lying atomic spin wave from single collective Rydberg excitation has been proposed as a potential candidate for realizing quantum computing [4, 5]. The interacted strength between two Rydberg atoms can be turned on and off with a contrast of 12 orders of magnitude by preparing the atoms to Rydberg states or not [6], which results in a significant advantage in realizing a C-NOT gate [7]. Moreover, the high-lying atomic spin wave is central to many other interesting applications such as efficient single-photon generation [8], exploration of the attractive interaction between single photons [9], preparation of entanglement between light and atomic excitations [10], all-optically switching operating using single-photon [11, 12], studying non-equilibrium phase transitions with many-body physics [13, 14]. A low-lying atomic spin wave consisting of metastable levels is suitable for quantum memory because of its long coherence time, a major barrier to long-distance quantum communication [15–22]. Regarded as disparate quantum systems, connecting the low- and high-lying atomic spin waves are crucially important in establishing long-

distance quantum communication [1, 15] and distributed quantum computation [23, 24]. In addition, developing quantum link between low- and high-lying atomic spin waves would make quantum networks work with superior scaling properties and have other advantages [6], such as the MHz-rate gate operations, more tolerance to some critical parameters: weak dependence on atomic motion, independence on the blockade shift and etc. Alternatively, such entanglement is very promising for studying dynamics behavior of entanglement under external perturbations, such as microwave and rf dressing. Demonstrating an entanglement between the two is therefore interesting and merits investigation.

In this letter, we report the development of a hybrid quantum link between two distant separated atomic ensembles through exciting a single-photon as a high-lying atomic spin wave. We first establish the entanglement between an anti-Stokes photon and a low-lying spin wave of one cold atomic ensemble by spontaneous Raman scattering (SRS). Next, we send this anti-Stokes photon to excite a high-lying atomic spin wave in another cold atomic ensemble. Via special designed interferometers, the low- and high-lying atomic spin waves are entangled in K-vector spaces. We demonstrate this entanglement by mapping them into two photons and checking their entanglement. We find that the Clauser-Horne-Shimony-Holt (CHSH) inequality is violated by more than nine standard deviations.

The medium for hybrid interface is optically thick ensembles of ⁸⁵Rb atoms trapped in two two-dimensional magneto-optical traps labeled MOT A and MOT B (Fig. 1(a)). The temperature of the atomic cloud in each is $\sim 200 \mu\text{K}$ and its size is $2 \times 2 \times 30 \text{ mm}^3$ [25]. The optical depths are 20 and 10 respectively. The hybrid quantum link involves two procedures: a) preparing an entangle-

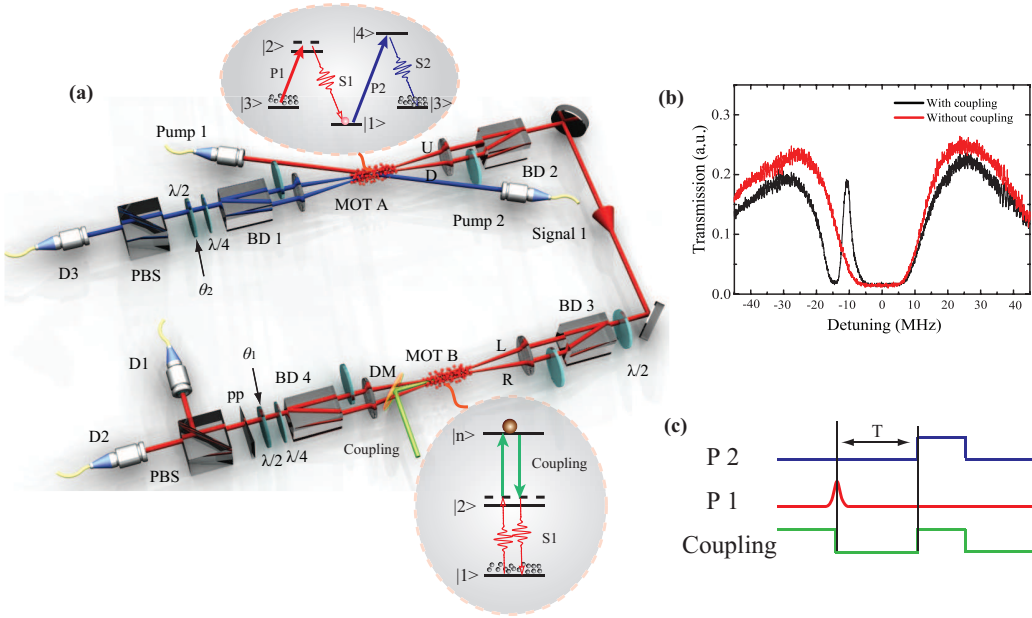


Figure 1. (a) Experimental setup and energy-level diagrams. The Rubidium energy levels dashed ellipses were used in storing signal 1 photon. $|1\rangle$ and $|3\rangle$ are atomic levels of $5S_{1/2}$ ($F=2$) and $5S_{1/2}$ ($F=3$). $|2\rangle$ and $|4\rangle$ are $5P_{1/2}$ ($F=3$) and $5P_{3/2}$ ($F=3$), respectively. $|n\rangle$ represents Rydberg state $nD_{3/2}$. DM: dichroic mirror. P_1, P_2 : pumps 1 and 2. S_1, S_2 : signal 1 and 2. M: mirror. BD: beam displacer. $\lambda/2$: half-wave plate. $\lambda/4$: quarter-wave plate. pp : the inserted phase plate. D1,2,3: single photon detectors. $\theta_{1,2}$ is defined as the angles of the half-wave plates inserted in the paths along which the signal 1 and signal 2 propagate, respectively. (b) Rydberg electromagnetically induced transparency (EIT). The horizontal axis stands for the detuning between the probe signal and the atomic transition from $5S_{1/2}$ ($F=2$) to $5P_{1/2}$ ($F=3$). In the experiment, the power of the coupling laser beam is 380 mW, beam size is of $\sim 19 \mu\text{m}$. The probe beam has a beam waist of $\sim 18 \mu\text{m}$. (c) Time sequence for demonstrating entanglement. T is the memory time of entanglement.

ment between a single photon and the low-lying atomic spin wave by SRS in MOT A and b) Storing single-photon as a high-lying atomic spin wave through EIT. The experiment was run periodically with a MOT trapping time of 7.5 ms and an experiment operating time of 1.5 ms, which contained 3,000 operation cycles of storage, each cycle a period of 500 ns (see time sequence in Fig. 1 (c)). Another 1 ms was used to prepare atoms to the initial atomic state $|3\rangle$ in MOT A, and state $|1\rangle$ in MOT B.

The signal-1 photon is prepared by atomic SRS process, which is correlated with the low-lying atomic spin wave $|a_{low}\rangle = 1/\sqrt{m} \sum_{i=1}^m e^{i\mathbf{k}_S \cdot \mathbf{r}_i} |3\rangle_1 \cdots |1\rangle_i \cdots |3\rangle_m$ in \mathbf{k}_S vector direction, where $\mathbf{k}_S = \mathbf{k}_{p1} - \mathbf{k}_{s1}$ is the wave vector of the low-lying atomic spin wave, \mathbf{k}_{p1} and \mathbf{k}_{s1} are the vectors of pump 1 and signal 1 fields, \mathbf{r}_i denotes the position of the i -th atom in atomic ensemble. Through storing signal-1 photon through Rydberg EIT (see Fig. 1(b)), a high-lying atomic spin wave $|a_{high}\rangle = 1/\sqrt{m} \sum_{i=1}^m e^{i\mathbf{k}_R \cdot \mathbf{r}_i} |1\rangle_1 \cdots |n\rangle_i \cdots |1\rangle_m$ is realized, where $\mathbf{k}_R = \mathbf{k}_C - \mathbf{k}_{s1}$ is the wave vector of the high-lying atomic spin wave, \mathbf{k}_C is the vector of coupling field, \mathbf{r}_i denotes the position of the i -th excited Rydberg atom in atomic ensemble. This new-type spin wave involves a highly lying excited atom, showing a special difference from low-lying atomic spin wave, for example the atomic size scales as $\sim n^2 \alpha_0$ (α_0 is the bohr radius, n de-

notes the principal quantum number of Rydberg atom). Finally, we establish the non-classical correlation between the low- and high-lying atomic spin waves. In this process, in order to build up the non-classical correlation between these two spin waves, small detuning ~ -10 MHz (see EIT spectrum in Fig. 1(b)) is used to match the $\sim +10$ MHz signal-1 photon. The reason to go off resonance is to reduce spontaneous emission noise in generating signal 1 field, not larger detunings is to maintain the EIT visibility. The detected signal-1 photons before and after memory are shown in Fig. 2(a), the storage efficiency after a programmed storage time of 300 ns is $\sim 22.9\%$. In principle, the storage efficiency can be further improved by optimizing the optical depth of atoms, the Rabi frequency of the coupling laser, the pulse profile of signal-1 photon and the bandwidth matching between storage media and signal-1 photon etc.

To check whether or not the non-classical property is retained during the storage, we map the low-lying and high-lying atomic spin waves to the signal-1 and signal-2 photons by opening the pump 1 and coupling pulses again after a programmed time, and check whether the Cauchy-Schwarz inequality was violated or not [18]. Classical light satisfies $R = [g_{s1,s2}(t)]^2 / g_{s1,s1}(t)g_{s2,s2}(t) \leq 1$, where $g_{s1,s2}(t)$ is the normalized second-order cross-correlation between signal-1 and signal-2 photons, $g_{s1,s1}(t)$, and

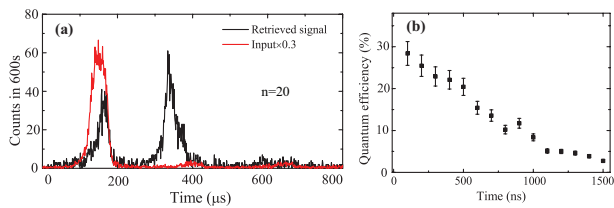


Figure 2. (a) Detecting heralded signal-1 photons with storage time of 300 ns. The storage efficiency is 22.9%. (b) The memory efficiency vs storage time at $n = 20$.

$g_{s2,s2}(t)$ are the corresponding auto-correlation of signal-1 and signal-2 photons respectively. In our experiment, $R \geq 43.2 \pm 7.3$ is obtained by using the measured auto-correlations $g_{s1,s1}(t) = 1.64$, $g_{s2,s2}(t) = 1.80$, the Cauchy-Schwarz inequality was strongly violated, clearly demonstrating the preservation of non-classical correlation during the storage of signal 1 photon in MOT B.

The storage efficiency against storage time is shown in Fig. 2(b). We estimate the dephasing time from Doppler decoherence is of $\sim 4.28 \mu\text{s}$ with considering the vector mismatch: $\Delta k = k_{475} - k_{795}$ and the velocity of the excited Rydberg atoms of 0.276 m/s. Thus, the Doppler decoherence and the lifetime of the Rydberg state ($n = 20$, with lifetime $\sim 5 \mu\text{s}$) are not the main limitations. The additional dephasing is maybe contributed from the perturbation of external fields.

We also characterized the single photon property of the signal 1 photon before and after storage by checking a heralded auto-correlation parameter $g_{s1;s1/s2}(t) = P_2 P_{213} / P_{21} P_{23}$, which is Hanbury-Brown and Twiss (HBT) experiment on triggered signal 1 photon [19, 26]. P_2 is the count of signal-2 photons; P_{21} and P_{23} are the two-fold coincidence counts between the signal-2 photons and the two separated signal-1 photons respectively; and P_{213} is the three-fold coincidence counts between the signal-2 photons and the two separated signal-1 photons. A pure single photon has $g_{s1;s1/s2}(t) = 0$ and a two-photon state has $g_{s1;s1/s2}(t) = 0.5$. Therefore $g_{s1;s1/s2}(t) < 1.0$ violates the classical limit and $g_{s1;s1/s2}(t) < 0.5$ suggests the near-single-photon character. We obtained $g_{s1;s1/s2}(t)$ of 0.12 ± 0.02 of the input single photons and $g_{s1;s1/s2}(t)$ is 0.10 ± 0.01 of retrieved single photons, both closed to zero confirmed clearly the preservation of the single-photon nature in storage, i.e., showed definitively single high-lying atomic spin wave in MOT B. In Refs. [8] and [27], the input light field is a coherent light and a single high-lying atomic spin wave is prepared via Rydberg interactions within a blockade radius, which is confirmed by post-detecting the read-out photons. Here, the single high-lying atomic spin wave is achieved by absorbing heralded single photon.

At first, we realized the which-path entanglement of a heralded high-lying atomic spin wave in a specially designed interferometer, which can be written as

$$|\psi_1\rangle = \frac{1}{\sqrt{2}}(|0_R\rangle |1_L\rangle + e^{i\phi} |1_R\rangle |0_L\rangle) \quad (1)$$

where subscript L and R refer to the left and right optical paths in the interferometer, ϕ denotes the relative phase between these two optical modes, which is set to zero, and $|0\rangle$ and $|1\rangle$ denote number states of high-lying atomic spin wave, respectively. The entangled properties can be characterized by the reduced matrix density ρ on the basis of $|n_L\rangle$ and $|m_R\rangle$ with $\{n, m\} = \{0, 1\}$ [16]:

$$\rho = \frac{1}{P} \begin{pmatrix} p_{00} & 0 & 0 & 0 \\ 0 & p_{10} & d & 0 \\ 0 & d^* & p_{01} & 0 \\ 0 & 0 & 0 & p_{11} \end{pmatrix} \quad (2)$$

where p_{ij} is the probability of finding i high-lying atomic spin waves in mode L and j high-lying atomic spin waves in mode R (see Table 1); d is equal to $V(p_{01} + p_{10})/2$; and V is the visibility of the interference between modes L and R [see Fig. 3(b)]. Fig. 3(a) is the input signal-1 interference between modes L and R . P is the total probabilities: $P = p_{00} + p_{10} + p_{01} + p_{11}$. To characterize the entanglement properties, we use the concurrence [28] $Con = \frac{1}{P} \max(0, 2|d| - 2\sqrt{p_{00}p_{11}})$, which takes values between 0 and 1 representing extremes corresponding to a separable state and a maximally entangled state. To obtain the concurrence of the entangled state corresponding to equation (2), we read the high-lying atomic spin wave into a single-photon state. We measured the different probabilities, and calculated the concurrence to be $(3.39 \pm 0.5) \times 10^{-3}$ including all losses, thereby demonstrating the which-path entanglement of a high-lying atomic spin wave. The heralded probabilities are about 3.3×10^{-3} with overall optical losses 94.6% including photon detection loss (50%), fiber coupling loss (30%), filtering losses 33.5% (two cavity filtering loss: 30%, one narrowband filter loss: 5%), two-photon excitation loss (77%). In principle, these losses can be reduced significantly by improving the transmittance of the filters and the storage efficiency.

In order to demonstrate the entanglement between low- and high-lying atomic spin waves, we use an intrinsically stable interferometer consisted of two beam displacers (BD 1 and BD 2) to prepare the entanglement between signal-1 photon and the low-lying atomic spin wave in MOT A. In this configuration, due to the conservation of angular momentum in SRS process, the signal-1 photons with two linearly angular momentums (labeled as U and D directions in Fig. 1(a)) entangled with the low-lying atomic spin waves encoded in wave vectors $\mathbf{k}_{S,U} = \mathbf{k}_{p1} - \mathbf{k}_{s1,U}$ and $\mathbf{k}_{S,D} = \mathbf{k}_{p1} - \mathbf{k}_{s1,D}$. The form of the entanglement is:

$$|\psi_2\rangle = (|U_a\rangle |H_{s1}\rangle + e^{i\varphi} |D_a\rangle |V_{s1}\rangle) / \sqrt{2} \quad (3)$$

Table I. Measurements of \bar{p}_{ij} and concurrences C before and after collective Rydberg excitation.

	\bar{P}_{00}	\bar{P}_{01}	\bar{P}_{10}	\bar{P}_{11}	C_{on}
\bar{p}_{input}	0.9516 ± 0.0008	$(2.61 \pm 0.04) \times 10^{-2}$	$(2.29 \pm 0.04) \times 10^{-2}$	$(2.6 \pm 0.4) \times 10^{-5}$	$(3.4 \pm 0.1) \times 10^{-2}$
ρ_{output}	0.9937 ± 0.0001	$(3.33 \pm 0.05) \times 10^{-3}$	$(2.98 \pm 0.05) \times 10^{-3}$	$(1.0 \pm 0.5) \times 10^{-6}$	$(3.39 \pm 0.5) \times 10^{-3}$

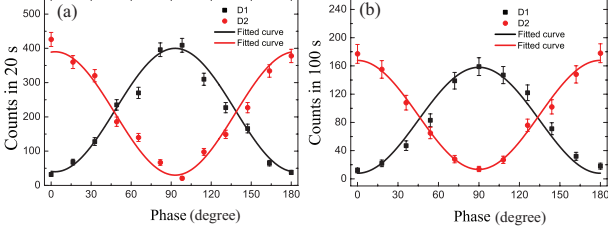


Figure 3. (a) Single-photon interference between L and R paths. (b) Single high-lying atomic spin wave interference with different phases between L and R paths, which is controlled by changing the phase of inserted phase plate (pp) which signal 1 photon passes. These counts are conditioned upon detection of signal 2 photon in path U . The visibilities of the interference curves in Fig. 3(a) and (b) are $90.6 \pm 0.4\%$ and $85.4 \pm 0.9\%$ respectively. The storage time is 300 ns.

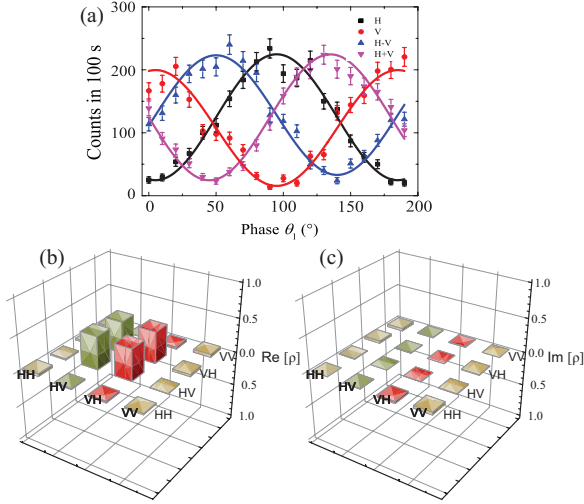


Figure 4. (a) The coincidences between signal-1 and signal-2 photons against the angle θ_1 of the HWP₁ through which signal 1 photon passes, where the signal 2 photon is detected in polarization direction of H , V , $H-V$ and $H+V$ respectively. The interference visibilities are $84.2\% \pm 1.0\%$, $87.8\% \pm 0.8\%$, $82.3\% \pm 1.2\%$, $81.6\% \pm 1.2\%$ respectively. (b) Real and (c) imaginary parts of the density matrices of the read-out entangled photonic state. The storage time is 300 ns.

with φ the relative phase between the upper and lower optical paths, which is set as zero in our experiment, $|U_a\rangle$ and $|D_a\rangle$ represents the low-lying atomic spin waves encoded in wave vectors $\mathbf{k}_{S,U}$ and $\mathbf{k}_{S,D}$ respectively. $|H_{s1}\rangle$ and $|V_{s1}\rangle$ denotes the horizontal and vertical polarized state of signal 1 photon. We next input the signal-1 pho-

tons into MOT B and subsequent stored it as a high-lying atomic spin wave. With the aid of a specially designed interferometer in MOT B, we established the entanglement between the low-lying atomic spin wave in MOT A and the high-lying atomic spin wave in MOT B, which can be expressed as:

$$|\psi_3\rangle = (|U_a\rangle |r_L\rangle + e^{i(\varphi+\theta)} |D_a\rangle |r_R\rangle) / \sqrt{2} \quad (4)$$

where $|r_L\rangle$ and $|r_R\rangle$ are the corresponding state of high-lying atomic spin wave encoded in $\mathbf{k}_{R,L} = \mathbf{k}_C - \mathbf{k}_{s1,L}$ and $\mathbf{k}_{R,R} = \mathbf{k}_C - \mathbf{k}_{s1,R}$ respectively.

If considering the low- and high-lying atomic spin waves individually, the state of each spin wave are both mixed in \mathbf{K} -vector spaces. However, the overall state of these two spin waves cannot be described independently, it is an entangled state. We checked this entanglement between them by mapping the atom-atom entanglement into the photon-photon polarization entanglement. By detecting the signal 2 photon in the polarization direction of $|H\rangle$, $|V\rangle$, $|H-V\rangle$, and $|H+V\rangle$ respectively, we record the coincidence rates between signal-1 and signal-2 photons against the angle θ_1 of the HWP₁ through which signal 1 photon passes, and plot the two-photon interference curves (shown in Fig. 4(a)). All visibilities are better than the threshold of 70.7% that is the benchmark of Bell's inequality, showing that entanglement has been preserved during storage. We also used the well-known Bell-type CHSH inequality to check the entanglement. We define the S value as:

$$S = |E(\theta_1, \theta_2) - E(\theta_1, \theta'_2) + E(\theta'_1, \theta_2) + E(\theta'_1, \theta'_2)| \quad (5)$$

where θ_1 and θ_2 are angles of the inserted half-wave plates shown in Fig. 1, and the different $E(\theta_1, \theta_2)$ are calculated using

$$E(\theta_1, \theta_2) = \frac{C(\theta_1, \theta_2) + C(\theta_1 + \frac{\pi}{2}, \theta_2 + \frac{\pi}{2}) - C(\theta_1 + \frac{\pi}{2}, \theta_2) - C(\theta_1, \theta_2 + \frac{\pi}{2})}{C(\theta_1, \theta_2) + C(\theta_1 + \frac{\pi}{2}, \theta_2 + \frac{\pi}{2}) + C(\theta_1 + \frac{\pi}{2}, \theta_2) + C(\theta_1, \theta_2 + \frac{\pi}{2})} \quad (6)$$

The angles of $\theta_1=0$, $\theta_2=\pi/8$, $\theta'_1=\pi/4$, and $\theta'_2=3\pi/8$. The S value we obtained is 2.29 ± 0.03 . All experimental data including two-photon visibilities and the S value suggests that there is an entanglement between low- and high-lying atomic spin waves. We also performed two-qubit tomography on the read-out photons of signal 1 and signal 2. The reconstructed density matrix (Fig. 4(a) and

Fig. 4(b)), when compared with the ideal density matrix of the maximally entangled state, yields a calculated fidelity of $89.4 \pm 2.6\%$. We conclude again that entanglement between the low- and high-lying atomic spin waves existed in the separated atomic ensembles.

In summary, we reported on an experiment where we have constructed a hybrid interface between two separate atomic systems. We have demonstrated two different entangled states in our experiment: which-path entanglement of a high-lying atomic spin wave and the entanglement between a high-lying atomic spin wave and a low-lying atomic spin wave. These two entanglements are totally different because of their corresponding to single-particle and two-particle independently separated quantum states. The entanglement established between low- and high-lying atomic spin waves in two atomic ensembles is physically separated 1 meter apart. With the high-lying atomic spin wave being highly sensitive to external perturbations such as stray electric fields and blackbody radiation, thus this hybrid entanglement shows many prospective projects on sensing external perturbation. Moreover, via dipole interaction between Rydberg atoms, one can in principle demonstrate blocking or switching photonic entanglement based on such a system. Our results in establishing two atomic spin waves with different scales show promise for advances in the field of quantum information science and fundamental studies in quantum physics, especially in constructing Rydberg-based quantum networks.

We very much thank Wei-bin Li, Lu-Ming Duan, Zheng-Wei Zhou and Yong-Jian Han for helpful discussions. This work was funded by the National Natural Science Foundation of China (Grant Nos. 11174271, 61275115, 61435011, 61525504).

* dds@ustc.edu.cn

† drshi@ustc.edu.cn

- [1] H. J. Kimble, *Nature* **453**, 1023 (2008).
- [2] A. Gaëtan, Y. Miroshnychenko, T. Wilk, A. Chotia, M. Viteau, D. Comparat, P. Pillet, A. Browaeys, P. Grangier, *et al.*, *Nature Physics* **5**, 115 (2009).
- [3] E. Urban, T. A. Johnson, T. Henage, L. Isenhower, D. Yavuz, T. Walker, and M. Saffman, *Nature Physics* **5**, 110 (2009).
- [4] D. Jaksch, J. Cirac, P. Zoller, S. Rolston, R. Côté, and M. Lukin, *Physical Review Letters* **85**, 2208 (2000).
- [5] M. Lukin, M. Fleischhauer, R. Cote, L. Duan, D. Jaksch, J. Cirac, and P. Zoller, *Physical Review Letters* **87**, 037901 (2001).
- [6] M. Saffman, T. Walker, and K. Mølmer, *Reviews of Modern Physics* **82**, 2313 (2010).
- [7] L. Isenhower, E. Urban, X. Zhang, A. Gill, T. Henage, T. A. Johnson, T. Walker, and M. Saffman, *Physical review letters* **104**, 010503 (2010).
- [8] Y. Dudin and A. Kuzmich, *Science* **336**, 887 (2012).
- [9] O. Firstenberg, T. Peyronel, Q.-Y. Liang, A. V. Gorshkov, M. D. Lukin, and V. Vuletić, *Nature* **502**, 71 (2013).
- [10] L. Li, Y. Dudin, and A. Kuzmich, *Nature* **498**, 466 (2013).
- [11] S. Baur, D. Tiarks, G. Rempe, and S. Dürr, *Physical review letters* **112**, 073901 (2014).
- [12] H. Gorniaczyk, C. Tresp, J. Schmidt, H. Fedder, and S. Hofferberth, *Physical review letters* **113**, 053601 (2014).
- [13] C. Carr, R. Ritter, C. Wade, C. S. Adams, and K. J. Weatherill, *Physical review letters* **111**, 113901 (2013).
- [14] D. Ding, C. Adams, B. Shi, and G. Guo, arXiv preprint arXiv:1606.08791 (2016).
- [15] L.-M. Duan, M. Lukin, J. I. Cirac, and P. Zoller, *Nature* **414**, 413 (2001).
- [16] K. S. Choi, H. Deng, J. Laurat, and H. Kimble, *Nature* **452**, 67 (2008).
- [17] A. Radnaev, Y. Dudin, R. Zhao, H. Jen, S. Jenkins, A. Kuzmich, and T. Kennedy, *Nature Physics* **6**, 894 (2010).
- [18] A. Kuzmich, W. Bowen, A. Boozer, A. Boca, C. Chou, L.-M. Duan, and H. Kimble, *Nature* **423**, 731 (2003).
- [19] T. Chaneliere, D. Matsukevich, S. Jenkins, S.-Y. Lan, T. Kennedy, and A. Kuzmich, *Nature* **438**, 833 (2005).
- [20] H. Zhang, X.-M. Jin, J. Yang, H.-N. Dai, S.-J. Yang, T.-M. Zhao, J. Rui, Y. He, X. Jiang, F. Yang, *et al.*, *Nature Photonics* **5**, 628 (2011).
- [21] D.-S. Ding, W. Zhang, Z.-Y. Zhou, S. Shi, G.-Y. Xiang, X.-S. Wang, Y.-K. Jiang, B.-S. Shi, and G.-C. Guo, *Physical review letters* **114**, 050502 (2015).
- [22] D.-S. Ding, W. Zhang, Z.-Y. Zhou, S. Shi, B.-S. Shi, and G.-C. Guo, *Nature Photonics* **9**, 332 (2015).
- [23] L.-M. Duan and C. Monroe, *Reviews of Modern Physics* **82**, 1209 (2010).
- [24] R. Van Meter, T. D. Ladd, A. G. Fowler, and Y. Yamamoto, *International Journal of Quantum Information* **8**, 295 (2010).
- [25] L. Yang, W. Jing-Hui, S. Bao-Sen, and G. Guang-Can, *Chinese Physics Letters* **29**, 024205 (2012).
- [26] P. Grangier, G. Roger, and A. Aspect, *EPL (Europhysics Letters)* **1**, 173 (1986).
- [27] D. Maxwell, D. Szwed, D. Paredes-Barato, H. Busche, J. Pritchard, A. Gauguet, K. Weatherill, M. Jones, and C. Adams, *Physical review letters* **110**, 103001 (2013).
- [28] W. K. Wootters, *Physical Review Letters* **80**, 2245 (1998).